

pubs.acs.org/Macromolecules Article

Ultrasound-Assisted RAFT Polymerization in a Continuous Flow Method

Amrish Kumar Padmakumar, Nikhil K. Singha, Muthupandian Ashokkumar, Frank A. Leibfarth,* and Greg G. Qiao*



Cite This: *Macromolecules* 2023, 56, 6920–6927



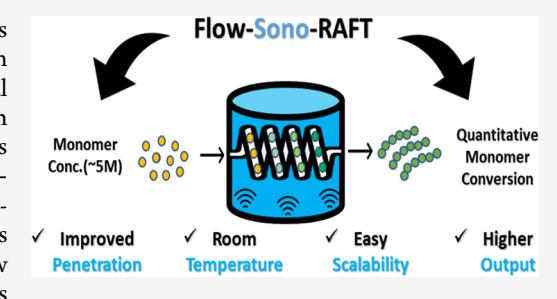
ACCESS I

III Metrics & More

Article Recommendations

Supporting Information

ABSTRACT: Developments in nanomolecular engineering in the last 20 years have led to the development of technology that uses ultrasonic irradiation in initiating the polymerization process for wider industrial and commercial applications. In this experimental study, ultrasound-assisted reversible addition chain-transfer (Sono-RAFT) polymerization was used to differentiate the effects of the bulk and continuous flow polymerization methods on three parameters—monomer conversion, polymer molar mass, and dispersity—using 2-hydroxyethyl acrylate, N-acryloyl morpholine, and N-dimethylacetamide as monomer substrates. Experimental results indicate that continuous flow polymerization demonstrated higher monomer conversion than polymerizations



performed in batch under identical experimental conditions. Furthermore, the increased surface-to-volume ratio inherent to continuous flow reactors enabled Sono-RAFT at a higher monomer concentration than analogous batch reactions due to the higher cavitational intensity accessible in tubular microreactors. The key to continuous flow Sono-RAFT was the observation that stainless-steel microreactors result in increased cavitational intensity and decreased oxygen contamination compared to PFA tubing. We envision that these findings will further advance the field of mechanochemistry in polymer science and provide an approach to make sonochemically regulated polymerization more practical and sustainable.

INTRODUCTION

In the recent two decades, advances in radical polymerization have resulted in versatile synthetic methods termed reversible deactivation radical polymerization (RDRP). 1-4 In contrast to conventional polymerization methods, RDRP enables fine control over the molar mass and dispersity of the finished polymer product. Free-radical species that create an equilibrium between active and dormant chain ends aid in the development of polymer chains in the RDRP process. The state of near equilibrium facilitates the simultaneous growth of all chains, leading to the production of polymers that possess a defined molar mass and a narrow molecular weight distribution. The polymerization process, due to its versatility and precision, has led to the rapid expansion of research in the field of RDRP, 5-8 which holds significant potential for various industrial and technological applications. Reversible additionfragmentation chain-transfer (RAFT) polymerization,9 atom transfer radical polymerization (ATRP), 15-26 and nitroxide-mediated polymerization^{27–31} are the commonly used RDRP techniques.

Traditionally, RAFT polymerization is initiated using thermal energy, ^{32,33} light, ^{34,35} enzyme, ^{36,37} redox, ^{38,39} and magnetic field. ^{40,41} We recently developed a method to initiate RAFT polymerization using ultrasonic irradiation to generate a low concentration of radicals. ⁴² The application of ultrasound in polymerization processes is a versatile technique that can be

utilized across a diverse array of monomers, 42-49 solvents, 50-52 and polymerization methodologies. These include free-radical polymerization, 53-55 ring-opening polymerization, 56,57 and RDRP,⁵⁸⁻⁶¹ among others. Uses for ultrasound range from medical imaging 62 and sewage treatment 63 to the creation of drug carriers 64 and the dehydration of food and dairy products.65 The aforementioned outcomes are attained through diverse ultrasound modalities, including but not limited to cavitation, vibration, radiation, acoustic scattering, and acoustic streaming.⁶⁶ Ultrasound-assisted RAFT (Sono-RAFT) generates cavitation in water, which stimulates water sonolysis and generates several physicochemical changes, including radical generation. 42–44,51,61,67 When rarefactive negative pressure exceeds the attractive forces between water molecules, a cavity forms, which is filled with solvent vapor, dissolved gas, or both. The cavities continue to grow until they form large cavitation bubbles, which expand to unstable sizes until they violently collapse, generating zones and shock waves of high temperatures. A portion of the water molecules that

Received: April 26, 2023 Revised: July 25, 2023 Published: August 22, 2023





Scheme 1. Schematic Representation of the Synthesis of PolyHEA via Sono-RAFT

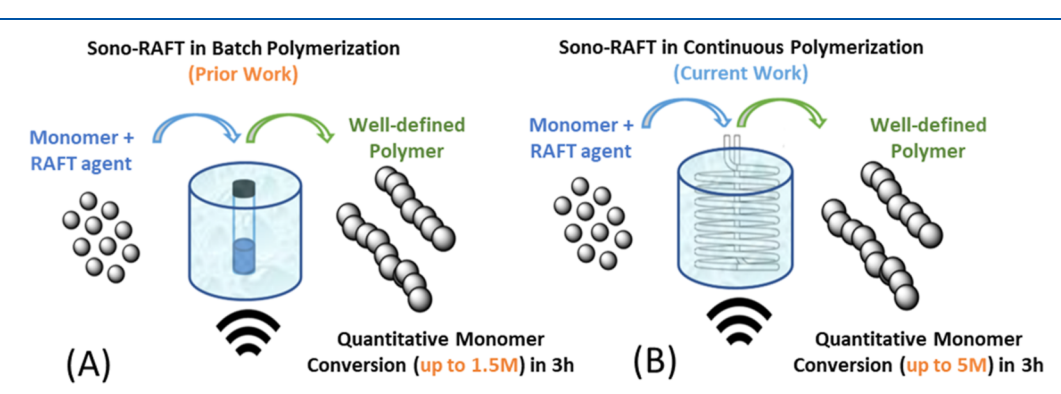


Figure 1. (A) In batch Sono-RAFT polymerization, the viscosity effects in the bulk medium causes reduction of cavitational intensity, thereby preventing the attainment of quantitative monomer conversions in reaction solutions that exceed 1.5 M. (B) The present study employs stainless-steel tubing to improve surface area and enhance cavitational intensity, resulting in quantitative monomer conversions of up to 5 M.

pass through these cavitation bubbles are decomposed into hydrogen (*H) and hydroxyl (*OH) radicals. These hydroxyl radicals subsequently initiate the polymerization reaction in the presence of a RAFT agent and a monomer (Scheme 1).⁴² As a result, depending on the ultimate use, a suitable frequency and power should be selected. Factors that increase radical production include increases in temperature, pressure, applied power, and frequency.⁶⁸ A steady supply of radical species is generated in Sono-RAFT reactions to achieve quantitative monomer conversions, chain activation, and good chain-end fidelity. In one sense, an adequate radical concentration can sustain a high reaction rate and monomer conversion within a given reaction time; on the other hand, the radical concentration must be low enough to minimize side reactions that generate dead chains. Ultrasound-mediated polymerization offers a number of benefits compared to thermal or photochemical processes, such as an accelerated polymerization rate and a lowered polymerization temperature. The utilization of ultrasound in polymerization reactions has been found to have several advantages. First, it allows for a reduction in reaction time due to the increased rate of reaction caused by cavitation. Moreover, tuning sonication conditions can modify the radical concentration in the solution either by changing the reaction frequency or by manipulating the applied power. Second, it has been observed to enhance the solubility of the reactants, leading to improved reaction kinetics. Third, the absence of external initiators or catalysis in ultrasound-assisted polymerization reactions results in a lower likelihood of byproduct formation and an increase in the yield of the polymer product. Lastly, the cavitation process induced by ultrasound generates a mechanical force that ensures better mixing and dispersion, which is beneficial in post-polymerization processing. The utilization of aqueous media for polymerization and the lack of external initiators or catalysts make ultrasound-mediated polymerization a sustainable process. Therefore, it is complementary with other mecha-

nisms, such as the photoiniferter RAFT process that is free of initiators or metal-free RDRP processes. \$1,66,67

A critical drawback of Sono-RAFT, however, is that poor cavitational efficiency at higher viscosity limits the approach to solutions of a low concentration. Evidence for this comes from our previous study, where polymers with a higher monomer concentration (>2.5 M) could not be synthesized using Sono-RAFT. 42 Therefore, methods that enable efficient Sono-RAFT polymerization at a high monomer concentration (i.e., >3 M) are desirable. Polymerization conducted in continuous reactors is an emerging area of research and practice due to the reproducible control of reaction conditions, improved mass and heat transfer, and ease of scale-up. 11,69,70 Early and contemporary work has demonstrated that RAFT polymerization is well-suited for continuous flow processes. hypothesized that the high surface-to-volume ratio inherent to the tubular reactors used in continuous flow polymerization could provide a strategy to enhance the cavitational intensity of sonochemistry and thus enable Sono-RAFT to proceed at higher concentrations than were possible in the corresponding batch process.

Herein, we describe the synthesis of a diverse range of polymers at a high monomer concentration (>3 M) using Sono-RAFT polymerization in a flow reactor. The high surfaceto-volume ratio of tubular reactors enabled access to higher cavitational intensity in the polymerization solution, which enabled Sono-RAFT at higher concentrations than possible in previously reported batch processes (Figure 1). A degassing procedure that leverages oxygen consumption by glucose oxidase (GOx)¹² provided general reaction conditions for the polymerization of hydroxyethyl acrylate (HEA), N-acryloyl morpholine (NAM), and N,N-dimethylacrylamide (DMA) in tubular reactors. We envision the ability to conduct Sono-RAFT under translationally relevant conditions as well as the understanding of how the reactor surface area influences sonochemical reactions will be of value to the polymer science community.

Table 1. Theoretical and Observed Molecular Weights under N2 and GOx Degassing Methods

		b	oatch—N ₂ degass	ed		batch—GOx degassed				
[M]	DP_n	monomer conversion (%)*	$\operatorname{Mn_{Theo}}_{(g \text{ mol}^{-1})^a}$	${\operatorname{Mn}_{\operatorname{Obs}} \atop (\operatorname{g} \operatorname{mol}^{-1})^b}$	Đ	monomer conversion $\operatorname{Mn_{Theo}}_{(\%)^*}$ $(g \operatorname{mol}^{-1})^a$		$(g \text{ mol}^{-1})^{b}$ \mathcal{D}		time (h)
1.0 M	100	98	11,700	11,700	1.01	98	11,700	11,300	1.02	3
3.0 M	100	71	8500	8200	1.04	89	10,600	10,400	1.03	3
5.0 M	100	50	6100	5900	1.21	77	9200	9600	1.08	3

^aDefined as $M_{n,\text{th}} = (\text{conv.} \times \text{DP}_n) \times \text{MW}_{\text{mon}} + \text{MWTTC}$, where $\text{DP}_n = [\text{HEA}]_0/[\text{TTC}]_0$. ^bCalculated via GPC-MALS using ASTRA software. *Determined via ¹H NMR spectroscopy.

■ RESULTS AND DISCUSSION

Batch Polymerization. Polymerization of the HEA using Sono-RAFT resulted in the synthesis of poly(2-hydroxyethyl

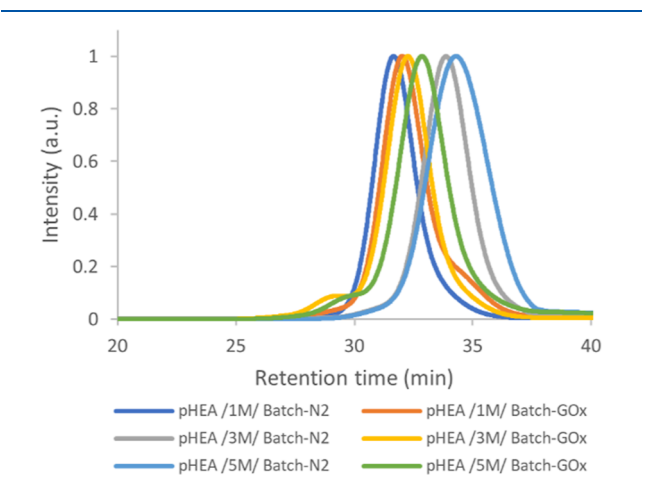


Figure 2. GPC chromatograms of polyHEA in water at room temperature carried out in a batch method with degassing by nitrogen (N_2) and GOx.

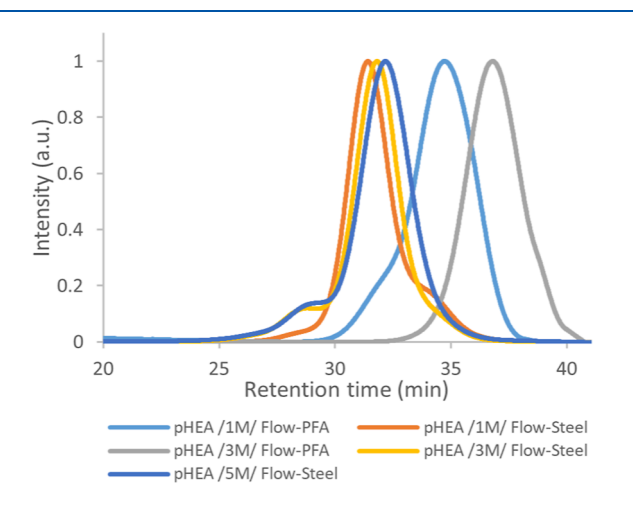


Figure 3. GPC chromatograms of chain extensions of polyHEA in water at room temperature carried out in the continuous flow method in PFA and SS microreactors.

acrylate) under batch conditions. Two methods were evaluated to remove oxygen from the reaction solution—sparging with nitrogen gas or degassing using the reaction of GOx along with glucose. At a degree of polymerization (DP) of 100 and a reaction time of 3 h, the effect of the two strategies was compared in terms of monomer conversion, polymer molar mass, and dispersity. As indicated in our early work, ^{42,52} the concentration of the OH radical in the system was measured

via spectroscopic technique. The monomer conversion was higher in experiments carried out with GOx degassing compared to N_2 degassing (Table 1). In both degassing methods, the observed molar masses closely matched those of the theoretical molar masses of polyHEA invariate of concentration (Table 1). HEA may interact strongly with the stationary phase of a chromatographic column. These interactions can cause the compound to adsorb more strongly to the stationary phase, resulting in slower elution and tailing peaks (Figure 2).

Oxygen can inhibit the polymerization reaction, resulting in a polymer with a lower molar mass and a slower rate of monomer conversion. GOx degassing is more effective at removing oxygen because GOx removes oxygen by converting glucose to gluconic acid and hydrogen peroxide, which reacts with oxygen to form water and oxygen. This reaction helps maintain a low oxygen concentration throughout the reaction by removing oxygen from the reaction solution. Experiments with GOx degassing revealed a higher monomer conversion rate than those with N2 degassing (Table 1). This suggests that GOx is more effective at removing oxygen from the reaction solution, resulting in a more thorough polymerization of the monomers. Consequently, GOx was used to conduct degassing for all subsequent reactions.

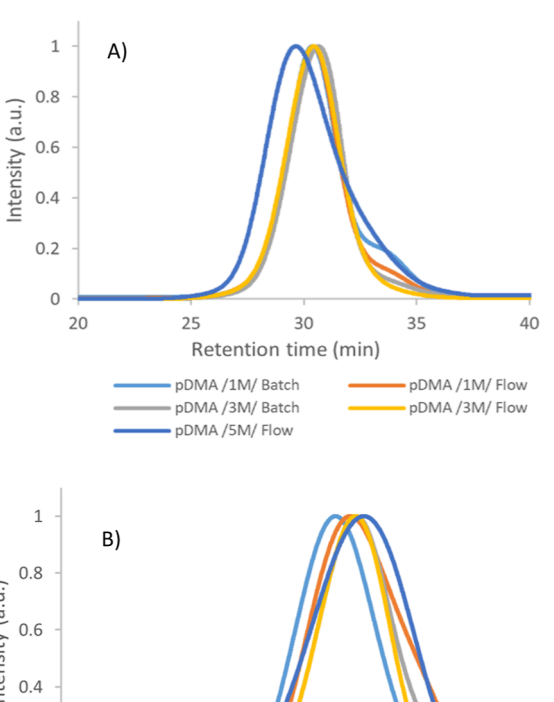
Continuous Polymerization. We sought to test our hypothesis that the higher surface-to-volume ratio in tubular reactors would improve cavitational flux and thereby improve the ability to synthesize polymers via Sono-RAFT with a higher monomer concentration. To begin, polymerization of HEA was conducted in either PFA or SS microreactors. PFA is the most popular material for flow polymerization reactors due to its flexibility and transparency. Sono-RAFT reactions are extraordinarily sensitive to oxygen, but oxygen diffusion through PFA tubes is substantial.^{24–28} This is evident from the significant decreases in monomer conversion observed between PFA tubular reactors and steel reactors (Figure 3). Moreover, these effects were more pronounced at higher monomer concentrations (Table 2). We hypothesized that the material properties of PFA account for the lower yields. PFA is susceptible to oxygen permeation, thereby increasing the likelihood of chain-end reduction and polymerization termination. In addition, elastic PFA tubing attenuates ultrasound, which decreases the cavitational intensity, particularly at higher monomer concentrations (>3 M). While the continuous flow method increases the surface area of the reaction vessel, the inability of PFA tubing to leverage this benefit and maintain the maximum cavitational intensity indicates that PFA is not the optimal material for the Sono-RAFT reactions.

We were motivated to investigate the use of SS for continuous polymerization due to the fact that steel resonates sound waves, which could potentially enhance the acoustic cavitation of the reaction. The steel tubing focuses the sound

Table 2. Theoretical and Observed Molecular Weights of PolyHEA in PFA and SS Microreactors

		cc	ontinuous flow—I	PFA		continuous flow—steel				
[M]	DP_n	monomer conversion (%)*	$\operatorname{Mn_{Theo}}_{(g \text{ mol}^{-1})^a}$	${\operatorname{Mn}_{\operatorname{Obs}} \atop (\operatorname{g} \operatorname{mol}^{-1})^b}$	Đ	monomer conversion (%)*	$\operatorname{Mn_{Theo}}_{(g \text{ mol}^{-1})^a}$	$(g \text{ mol}^{-1})^b$ D		time (h)
1 M	100	74	8900	8400	1.31	99	11,800	11,600	1.13	3
3 M	100	40	4900	4600	1.26	99	11,800	11,600	1.15	3
5 M	100					98	11,700	10,800	1.17	3

^aDefined as $M_{n,\text{th}} = (\text{conv.} \times \text{DP}_n) \times \text{MW}_{\text{mon}} + \text{MWTTC}$, where $\text{DP}_n = [\text{HEA}]_0/[\text{TTC}]_0$. ^bCalculated via GPC-MALS using ASTRA software. *Determined via ¹H NMR spectroscopy.



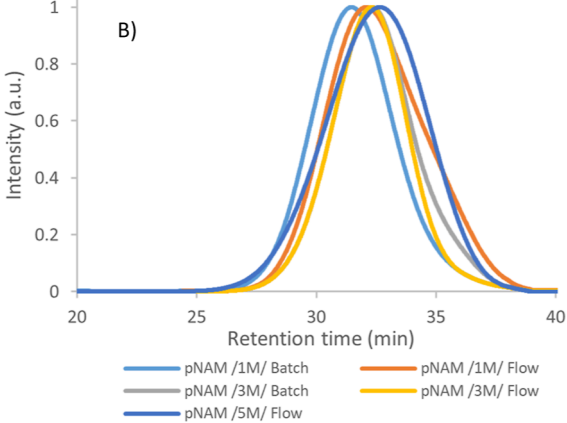


Figure 4. GPC chromatograms of chain extensions of polyDMA (A) and polyNAM (B) in water at room temperature carried out in the continuous flow method in the SS microreactor.

waves in a specific location, increasing the cavitation's intensity and enhancing the process's efficiency. In addition, the use of steel tubing can prevent the loss of ultrasonic energy that may occur if the liquid is allowed to spread out too much. The tubing can function as a waveguide, directing sound impulses into the liquid and allowing them to travel without significant attenuation. Unlike PFA tubing, stainless steel is neither transparent nor air-permeable, making it a highly desirable microreactor material. Overall, steel tubing can improve the efficacy of ultrasound cavitation by providing a more efficient and concentrated method for generating and controlling the cavitation process. According to our investigations, the Sono-RAFT polymerization of HEA under continuous flow conditions in a stainless-steel reactor resulted in quantitative monomer conversion at all measured concentrations, which is an improvement over batch reactions in a glass reactor (Table 2). These data are consistent with Hornung et al.'s observation that a SS microreactor provided better oxygen-free conditions and improved monomer conversions.⁷¹

Non-ideal conditions for the polymerization reaction may arise due to inadequate temperature control, poor mixing, or variations in reactant concentrations within the flow tube due to low flow rates. The presence of such conditions may enhance the probability of side reactions or modify the reaction kinetics, which could lead to the production of unintended products. Unlike batch polymerization, polymers produced via continuous flow indicated the presence of shoulder in the gel permeation chromatography (GPC) curves and the dispersity of these polymers were slightly higher than those produced by the batch method. It is hypothesized that the presence of shoulders in the GPC curves can be attributed to inhomogeneity in the flow process. In order to alleviate undesired reactions in flow tube polymerizations, it is crucial to careful optimize the reaction parameters such as the temperature regulation, reactant concentrations, applied power, ultrasound frequency, and residence time. 74,75 Furthermore, the judicious choice and configuration of the flow tube, coupled with effective mixing and reaction regulation, can mitigate the prevalence of undesired reactions.

Relative Effects of Batch and Continuous Flow Methods on Monomer Conversion. The present study aimed to evaluate the central hypothesis that the employment of continuous flow tubular reactors with a high surface-to-volume ratio would amplify the cavitational intensity of

Table 3. Theoretical and Observed Molecular Weights of PolyDMA in Batch and Continuous Flow Methods

		monomer conversion (%)*		batch			con			
[M]	DP_n	batch	flow	Mn _{Theo} (g mol ⁻¹) ^a	$\mathrm{Mn}_{\mathrm{Obs}}\ (\mathrm{g}\ \mathrm{mol}^{-1})^{b}$	Đ	Mn _{Theo} (g mol ⁻¹) ^a	$\mathrm{Mn}_{\mathrm{Obs}} \ (\mathrm{g} \ \mathrm{mol}^{-1})^{b}$	Đ	time (h)
1 M	100	93	99	9800	9700	1.06	10,100	9900	1.04	4
3 M	100	93	99	9500	9600	1.03	10,100	9800	1.03	4
5 M	100		98				10,000	11,300	1.27	4

[&]quot;Defined as $M_{n,\text{th}} = (\text{conv.} \times \text{DP}_n) \times \text{MW}_{\text{mon}} + \text{MWTTC}$, where $\text{DP}_n = [\text{HEA}]_0 / [\text{TTC}]_0$. "Calculated via GPC-MALS using ASTRA software. *Determined via ¹H NMR spectroscopy.

Table 4. Theoretical and Observed Molecular Weights of PolyNAM in Batch and Continuous Flow Methods

		monomer conversion (%)*			batch	continuous flow				
[M]	DP_n	batch	flow	Mn _{Theo} (g mol ⁻¹) ^a	Mn _{Obs} (g mol ⁻¹) ^b	Đ	Mn _{Theo} (g mol ⁻¹) ^a	Mn _{Obs} (g mol ⁻¹) ^b	Đ	time (h)
1 M	70	99	99	10,100	10,200	1.12	10,100	10,000	1.24	4
3 M	70	97	97	9800	9600	1.18	9800	9700	1.15	4
5 M	70		95				9600	9000	1.31	4

^aDefined as $M_{n,\text{th}} = (\text{conv.} \times \text{DP}_n) \times \text{MW}_{\text{mon}} + \text{MWTTC}$, where $\text{DP}_n = [\text{HEA}]_0/[\text{TTC}]_0$. ^bCalculated via GPC–MALS using ASTRA software. *Determined via ¹H NMR spectroscopy.

sonochemistry. We have calculated the surface areas of the batch and flow reactors, and they are 56.6 and 250.0 cm², respectively. The surface area of the flow reactor is approximately five times that of the batch reactor. Moreover, the introduction of ultrasonic waves into the batch reactor occurs via the bottom part of the vial, which possesses a reduced surface area in comparison to the flow reactor. Consequently, an increase in viscosity results in a decrease in cavitational intensity, which subsequently leads to a reduction in monomer conversion. The larger surface area affords more sites for bubble nucleation, resulting in more intense cavitation. In addition, they cause a greater number of reactant molecules to be exposed to the cavitational bubble, which increases reaction rates and conversion efficiencies. This, in turn, would facilitate the Sono-RAFT process to operate at elevated concentrations, surpassing the limits of the corresponding batch process.

Continuing from our prior work, these experiments were carried out in stainless-steel tubing under continuous flow conditions, utilizing GOx to remove oxygen from the solution. Polymerization of HEA was observed to occur across all concentrations evaluated (ranging from 1.0 to 5.0 M with respect to the monomer) under both batch and flow conditions. The experimental results indicate that the conversion of HEA in the batch mode exhibits a negative correlation with an increasing concentration, ultimately plateauing at 77% after a reaction time of 3 h at a concentration of 5.0 M. The monomer conversion of HEA during polymerization in continuous flow at 5.0 M was found to be 98%. This is believed to be a result of the increased cavitational intensity facilitated by the high surface-to-volume ratio of the tubular reactors. To understand if the benefits engendered by continuous flow are general, we explored this Sono-RAFT approach to other monomers, including DMA and NAM. For these two substrates, the positive influence of using tubular reactors is more pronounced.

Dispersity (D) is a measure of molecular weight distribution, and it is a very important parameter to determine the control and homogeneity of the polymerization reaction. At a lower monomer concentration (up to 3 M), the polymers produced via batch and continuous methods exhibit narrow and monomodal indicating well-controlled and homogeneous synthesis (Figure 4). Additionally, the observed molecular weight is identical to the theoretical molecular weight for both pDMA and pNAM. Due to the nature of the monomer, the dispersities of pDMA and pNAM at 5 M monomer concentrations were slightly higher compared to pHEA but still was measured to be less than 1.3. Nevertheless, as we increased the monomer concentration to 5 M in the batch method, the monomer conversion reduced significantly presumably due to the high viscosity of the medium and

therefore low cavitational intensity. In contrast, continuous flow conditions resulted in monomer conversions of 98 and 95% for pDMA and pNAM, respectively, at monomer concentrations of 5 M (Tables 3 and 4).

Clear trends emerge across the three monomers studied: the use of stainless-steel tubular reactors under continuous flow conditions enables Sono-RAFT polymerizations to proceed at a high monomer concentration. This is significant for the continued development and translation of Sono-RAFT because decreasing solvent usage reduces cost, minimizing solvent wasted enhances sustainability, and continuous production provides a pathway for scale-up that does not require excessively large ultrasound devices.

CONCLUSIONS

We report a continuous flow method for Sono-RAFT that has distinct advantages over the corresponding batch process. Most prominently, continuous flow Sono-RAFT enables polymerization at higher concentrations than in batch chemistry. The continuous flow Sono-RAFT polymerizations result in high monomer conversion and good agreement between the targeted and observed molar mass and dispersity values. Key to continuous flow Sono-RAFT was the observation that SS microreactors result in increased cavitational intensity and decreased oxygen contamination compared to PFA tubing. The benefits of continuous flow Sono-RAFT method were observed for all three monomers studied (HEA, DMA, NAM), which vary in both different structure and reactivity. The advancement of Sono-RAFT in the future is expected to involve the integration of automation and real-time monitoring into advanced continuous processes. These innovations aim to improve continuous polymerization control, efficiency, and sustainability even more. In addition, the investigation of new monomers, effect of reactor surface area, applied power, and frequency can result in the development of novel polymerization techniques with enhanced properties and a broader range of applications.

ASSOCIATED CONTENT

Supporting Information

The Supporting Information is available free of charge at https://pubs.acs.org/doi/10.1021/acs.macromol.3c00816.

Experimental section; weight sheet for Sono-RAFT reactions in batch and continuous flow methods; and ¹H NMR spectrum for polymers prepared via Sono-RAFT (PDF)

AUTHOR INFORMATION

Corresponding Authors

Frank A. Leibfarth — Department of Chemistry, University of North Carolina at Chapel Hill, Chapel Hill, North Carolina 27599, United States; orcid.org/0000-0001-7737-0331; Email: frankl@Email.unc.edu

Greg G. Qiao — Polymer Science Group, Department of Chemical Engineering, University of Melbourne, Parkville 3010, Australia; ⊙ orcid.org/0000-0003-2771-9675; Email: gregghq@unimelb.edu.au

Authors

Amrish Kumar Padmakumar – Polymer Science Group, Department of Chemical Engineering, University of Melbourne, Parkville 3010, Australia

Nikhil K. Singha – Rubber Technology Centre, Indian Institute of Technology, Kharagpur 721302, India; orcid.org/0000-0003-0935-0157

Muthupandian Ashokkumar — School of Chemistry, The University of Melbourne, Parkville 3010, Australia; orcid.org/0000-0002-8442-1499

Complete contact information is available at: https://pubs.acs.org/10.1021/acs.macromol.3c00816

Notes

The authors declare no competing financial interest.

ACKNOWLEDGMENTS

A.K.P. is grateful to Melbourne-India Postgraduate Program (MIPP) for the Melbourne Research Scholarship (MRS). N.K.S., M.A., and G.Q. gratefully acknowledge the financial support from Ministry of Education, India, under the Scheme for Promotion of Academic and Research Collaboration (SPARC) program (Ref. SPARC/2018-19/P136/SL).F.A.L. acknowledges the National Science Foundation under a CAREER award (CHE-1847362) for funding.

■ REFERENCES

- (1) Parkatzidis, K.; Wang, H. S.; Truong, N. P.; Anastasaki, A.; Anastasaki, A. Recent Developments and Future Challenges in Controlled Radical Polymerization: A 2020 Update. *Chem.* **2020**, *6*, 1575–1588.
- (2) Martinez, M. R.; Matyjaszewski, K. Degradable and Recyclable Polymers by Reversible Deactivation Radical Polymerization. *CCS Chem.* **2022**, *4*, 2176–2211.
- (3) Corrigan, N.; Jung, K.; Moad, G.; Hawker, C. J.; Matyjaszewski, K.; Boyer, C. Reversible-deactivation radical polymerization (Controlled/living radical polymerization): From discovery to materials design and applications. *Prog. Polym. Sci.* **2020**, *111*, 101311.
- (4) Gurnani, P.; Perrier, S. Controlled radical polymerization in dispersed systems for biological applications. *Prog. Polym. Sci.* **2020**, *102*, 101209.
- (5) Ren, J. M.; McKenzie, T. G.; Fu, Q.; Wong, E. H.; Xu, J.; An, Z.; Shanmugam, S.; Davis, T. P.; Boyer, C.; Qiao, G. G. Star polymers. *Chem. Rev.* **2016**, *116*, 6743–6836.
- (6) Carmean, R. N.; Becker, T. E.; Sims, M. B.; Sumerlin, B. S. Ultra-High Molecular Weights via Aqueous Reversible-Deactivation Radical Polymerization. *Chem.* **2017**, *2*, 93–101.
- (7) Engelis, N.; Anastasaki, A.; Nurumbetov, G.; Truong, N.; Nikolaou, V.; Shegiwal, A.; Whittaker, M.; Davis, T.; Haddleton, D. M. Sequence-controlled methacrylic multiblock copolymers via sulfurfree RAFT emulsion polymerization. *Nat. Chem.* **2017**, *9*, 171–178.
- (8) Gong, H.; Gu, Y.; Zhao, Y.; Quan, Q.; Han, S.; Chen, M. Precise Synthesis of Ultra-High-Molecular-Weight Fluoropolymers Enabled

- by Chain-Transfer-Agent Differentiation under Visible-Light Irradiation. *Angew. Chem.* **2020**, *132*, 929–937.
- (9) Moad, G.; Rizzardo, E.; Thang, S. H. RAFT polymerization and some of its applications. *Chem.—Asian J.* **2013**, *8*, 1634–1644.
- (10) Phommalysack-Lovan, J.; Chu, Y.; Boyer, C.; Xu, J. PET-RAFT polymerisation: towards green and precision polymer manufacturing. *Chem. Commun.* **2018**, *54*, 6591–6606.
- (11) Hatton, F. L. Recent advances in RAFT polymerization of monomers derived from renewable resources. *Polym. Chem.* **2020**, *11*, 220–229.
- (12) Zhang, T.; Yeow, J.; Boyer, C. A cocktail of vitamins for aqueous RAFT polymerization in an open-to-air microtiter plate. *Polym. Chem.* **2019**, *10*, 4643–4654.
- (13) McKenzie, T. G.; Fu, Q.; Uchiyama, M.; Satoh, K.; Xu, J.; Boyer, C.; Kamigaito, M.; Qiao, G. G. Beyond traditional RAFT: alternative activation of thiocarbonylthio compounds for controlled polymerization. *Adv. Sci.* **2016**, *3*, 1500394.
- (14) Nothling, M. D.; Fu, Q.; Reyhani, A.; Allison-Logan, S.; Jung, K.; Zhu, J.; Kamigaito, M.; Boyer, C.; Qiao, G. G. Progress and perspectives beyond traditional RAFT polymerization. *Adv. Sci.* **2020**, 7, 2001656.
- (15) Matyjaszewski, K. Atom transfer radical polymerization (ATRP): current status and future perspectives. *Macromolecules* **2012**, *45*, 4015–4039.
- (16) Siegwart, D. J.; Oh, J. K.; Matyjaszewski, K. ATRP in the design of functional materials for biomedical applications. *Prog. Polym. Sci.* **2012**, *37*, 18–37.
- (17) Krol, P.; Chmielarz, P. Recent advances in ATRP methods in relation to the synthesis of copolymer coating materials. *Prog. Org. Coat.* **2014**, *77*, 913–948.
- (18) Ding, M.; Jiang, X.; Zhang, L.; Cheng, Z.; Zhu, X. Recent progress on transition metal catalyst separation and recycling in ATRP. *Macromol. Rapid Commun.* **2015**, *36*, 1702–1721.
- (19) Wang, Z.; Pan, X.; Li, L.; Fantin, M.; Yan, J.; Wang, Z.; Wang, Z.; Xia, H.; Matyjaszewski, K. Enhancing mechanically induced ATRP by promoting interfacial electron transfer from piezoelectric nanoparticles to Cu catalysts. *Macromolecules* **2017**, *50*, 7940–7948.
- (20) Collins, J.; McKenzie, T.; Nothling, M.; Ashokkumar, M.; Qiao, G. G. High frequency sonoATRP of 2-hydroxyethyl acrylate in an aqueous medium. *Polym. Chem.* **2018**, *9*, 2562–2568.
- (21) Zaborniak, I.; Chmielarz, P. Ultrasound-Mediated Atom Transfer Radical Polymerization (ATRP). *Materials* **2019**, *12*, 3600.
- (22) Lorandi, F.; Matyjaszewski, K. Why do we need more active ATRP catalysts? *Isr. J. Chem.* **2020**, *60*, 108–123.
- (23) Truong, N. P.; Jones, G. R.; Bradford, K. G.; Konkolewicz, D.; Anastasaki, A. A comparison of RAFT and ATRP methods for controlled radical polymerization. *Nat. Rev. Chem* **2021**, *5*, 859–869.
- (24) Szczepaniak, G.; Fu, L.; Jafari, H.; Kapil, K.; Matyjaszewski, K. Making ATRP more practical: oxygen tolerance. *Acc. Chem. Res.* **2021**, 54, 1779–1790.
- (25) Wang, Y.; Lorandi, F.; Fantin, M.; Chmielarz, P.; Isse, A. A.; Gennaro, A.; Matyjaszewski, K. Miniemulsion ARGET ATRP via interfacial and ion-pair catalysis: From ppm to ppb of residual copper. *Macromolecules* **2017**, *50*, 8417–8425.
- (26) Zaborniak, I.; Chmielarz, P. Temporally controlled ultrasonication-mediated atom transfer radical polymerization in miniemulsion. *Macromol. Chem. Phys.* **2019**, 220, 1900285.
- (27) Sciannamea, V.; Jerome, R.; Detrembleur, C. In-situ nitroxide-mediated radical polymerization (NMP) processes: their understanding and optimization. *Chem. Rev.* **2008**, *108*, 1104–1126.
- (28) Grubbs, R. B. Nitroxide-mediated radical polymerization: limitations and versatility. *Polym. Rev.* **2011**, *51*, 104–137.
- (29) Petton, L.; Ciolino, A.; Stamenović, M.; Espeel, P.; Du Prez, F. E. From NMP to RAFT and Thiol-Ene Chemistry by In Situ Functionalization of Nitroxide Chain Ends. *Macromol. Rapid Commun.* **2012**, 33, 1310–1315.
- (30) Nicolas, J.; Guillaneuf, Y.; Lefay, C.; Bertin, D.; Gigmes, D.; Charleux, B. Nitroxide-mediated polymerization. *Prog. Polym. Sci.* **2013**, *38*, 63–235.

- (31) Audran, G.; Bagryanskaya, E. G.; Marque, S. R.; Postnikov, P. New variants of nitroxide mediated polymerization. *Polymers* **2020**, *12*, 1481.
- (32) Moad, G.; Rizzardo, E.; Thang, S. H. Living radical polymerization by the RAFT process. *Aust. J. Chem.* **2005**, *58*, 379–410.
- (33) Moad, G.; Chong, Y.; Mulder, R.; Rizzardo, E.; Thang, S. H. New Features of the Mechanism of RAFT Polymerization; ACS Publications, 2009.
- (34) Hartlieb, M. Photo-Iniferter RAFT Polymerization. *Macromol. Rapid Commun.* **2022**, 43, 2270003.
- (35) Lehnen, A.-C.; Kurki, J. A. M.; Hartlieb, M. The difference between photo-iniferter and conventional RAFT polymerization: high livingness enables the straightforward synthesis of multiblock copolymers. *Polym. Chem.* **2022**, *13*, 1537–1546.
- (36) Li, R.; Kong, W.; An, Z. Enzyme catalysis for reversible deactivation radical polymerization. *Angew. Chem.* **2022**, 134, No. e202202033.
- (37) Xie, W.; Zhao, L.; Wei, Y.; Yuan, J. Advances in enzyme-catalysis-mediated RAFT polymerization. *Cell Rep. Phys. Sci.* **2021**, 2, 100487.
- (38) Reyhani, A.; Logan, S. A.; Burachaloo, H. R.; McKenzie, T. G.; Bryant, G.; Qiao, G. G. Synthesis of ultra-high molecular weight polymers by controlled production of initiating radicals. *J. Polym. Sci., Part A: Polym. Chem.* **2019**, *57*, 1922–1930.
- (39) Reyhani, A.; McKenzie, T. G.; Fu, Q.; Qiao, G. G. Redoxinitiated reversible addition—fragmentation chain transfer (RAFT) polymerization. *Aust. J. Chem.* **2019**, *72*, 479–489.
- (40) Chiriac, A. Polymerization in a magnetic field. 14. Possibilities to improve field effect during methyl acrylate polymerization. *J. Appl. Polym. Sci.* **2004**, 92, 1031–1036.
- (41) Rintoul, I. Kinetic control of aqueous polymerization using radicals generated in different spin states. *Processes* **2017**, *5*, 15.
- (42) McKenzie, T. G.; Colombo, E.; Fu, Q.; Ashokkumar, M.; Qiao, G. G. Sono-RAFT Polymerization in Aqueous Medium. *Angew. Chem., Int. Ed.* **2017**, *S6*, 12302–12306.
- (43) Piogé, S.; Tran, T. N.; McKenzie, T. G.; Pascual, S.; Ashokkumar, M.; Fontaine, L.; Qiao, G. Sono-RAFT polymerization-induced self-assembly in aqueous dispersion: synthesis of LCST-type thermosensitive nanogels. *Macromolecules* **2018**, *51*, 8862–8869.
- (44) Wan, J.; Fan, B.; Liu, Y.; Hsia, T.; Qin, K.; Junkers, T.; Teo, B. M.; Thang, S. H. Room temperature synthesis of block copolymer nano-objects with different morphologies via ultrasound initiated RAFT polymerization-induced self-assembly (sono-RAFT-PISA). *Polym. Chem.* **2020**, *11*, 3564–3572.
- (45) Teo, B.; Prescott, S.; Price, G.; Grieser, F.; Ashokkumar, M. Synthesis of Temperature Responsive Poly(N-isopropylacrylamide) Using Ultrasound Irradiation. *J. Phys. Chem. B* **2010**, *114*, 3178–3184.
- (46) Teo, B. M.; Prescott, S. W.; Ashokkumar, M.; Grieser, F. Ultrasound initiated miniemulsion polymerization of methacrylate monomers. *Ultrason. Sonochem.* **2008**, *15*, 89–94.
- (47) Parra, C.; González, G.; Albano, C. Synthesis and characterization of poly (methyl methacrylate) obtained by ultrasonic irradiation. *E-Polymers* **2005**, *5*, 025.
- (48) Kobayashi, D.; Matsumoto, H.; Kuroda, C. Improvement of indirect ultrasonic irradiation method for intensification of emulsion polymerization process. *Chem. Eng. J.* **2008**, *135*, 43–48.
- (49) Bhanvase, B.; Sonawane, S. Ültrasound assisted in situ emulsion polymerization for polymer nanocomposite: A review. *Chem. Eng. Process* **2014**, *85*, 86–107.
- (50) Weissler, A.; Pecht, I.; Anbar, M. Ultrasound chemical effects on pure organic liquids. *Science* **1965**, *150*, 1288–1289.
- (51) Collins, J.; McKenzie, T.; Nothling, M.; Allison Logan, S.; Ashokkumar, M.; Qiao, G. G. Sonochemically Initiated RAFT Polymerization in Organic Solvents. *Macromolecules* **2019**, *52*, 185–195.

- (52) Padmakumar, A. K.; Kumar, A. R. S. S.; Allison-Logan, S.; Ashokkumar, M.; Singha, N. K.; Qiao, G. G. High chain-end fidelity in sono-RAFT polymerization. *Polym. Chem.* **2022**, *13*, 6140–6148.
- (53) Weissler, A. Formation of hydrogen peroxide by ultrasonic waves: free radicals. *J. Am. Chem. Soc.* **1959**, *81*, 1077–1081.
- (54) Riesz, P.; Berdahl, D.; Christman, C. L. Free Radical Generation by Ultrasound in Aqueous and Nonaqueous Solutions. *Environ. Health Perspect.* **1985**, *64*, 233–252.
- (55) Kojima, Y.; Koda, S.; Nomura, H.; Kawaguchi, S. Effect of sonication on nitroxide-controlled free radical polymerization of styrene. *Ultrason. Sonochem.* **2001**, *8*, 81–83.
- (56) Stoessel, S. The use of ultrasound to initiate ring-opening polymerization. J. Appl. Polym. Sci. 1993, 48, 505-507.
- (57) Price, G. J.; Lenz, E. J.; Ansell, C. W. The effect of high-intensity ultrasound on the ring-opening polymerisation of cyclic lactones. *Eur. Polym. J.* **2002**, *38*, 1753–1760.
- (58) Kubo, M.; Kondo, T.; Matsui, H.; Shibasaki-Kitakawa, N.; Yonemoto, T. Control of molecular weight distribution in synthesis of poly (2-hydroxyethyl methacrylate) using ultrasonic irradiation. *Ultrason. Sonochem.* **2018**, *40*, 736–741.
- (59) Kubo, M.; Sone, T.; Ohata, M.; Tsukada, T. Synthesis of poly (N-isopropylacrylamide-co-2-hydroxyethyl methacrylate) with low polydispersity using ultrasonic irradiation. *Ultrason. Sonochem.* **2018**, 49, 310–315.
- (60) McKenzie, T.; Karimi, F.; Ashokkumar, M.; Qiao, G. G. Ultrasound and Sonochemistry for Radical Polymerization: Sound Synthesis. *Chem.—Eur. J.* **2019**, *25*, 5372–5388.
- (61) Wan, J.; Fan, B.; Thang, S. H. Sonochemical preparation of polymer–metal nanocomposites with catalytic and plasmonic properties. *Nanoscale Adv.* **2021**, *3*, 3306–3315.
- (62) Lindner, J. Microbubbles in medical imaging: current applications and future directions. *Nat. Rev. Drug Discovery* **2004**, *3*, 527–533.
- (63) Ibáñez, M.; Lor, E. G.; Bijlsma, L.; Morales, E.; Pastor, L.; Hernández, F. M. Removal of emerging contaminants in sewage water subjected to advanced oxidation with ozone. *J. Hazard Mater.* **2013**, 260, 389–398.
- (64) Gao, Z.; Zhu, H.; Li, X.; Zhang, P.; Ashokkumar, M.; Cavalieri, F.; Hao, J.; Cui, J. Sono-polymerization of poly (ethylene glycol)-based nanoparticles for targeted drug delivery. *ACS Macro Lett.* **2019**, *8*, 1285–1290.
- (65) Ashokkumar, M.; Bhaskaracharya, R.; Kentish, S.; Lee, J.; Palmer, M.; Zisu, B. The ultrasonic processing of dairy products An overview. *Dairy Sci. Technol.* **2010**, *90*, 147—168.
- (66) Kumar, A. R. S. S.; Padmakumar, A.; Kalita, U.; Samanta, S.; Baral, A.; Singha, N. K.; Ashokkumar, M.; Qiao, G. G. Ultrasonics in polymer science: applications and challenges. *Prog. Mater. Sci.* **2023**, *136*, 101113.
- (67) Padmakumar, A. K.; Kumar, A. R. S. S.; Allison-Logan, S.; Ashokkumar, M.; Singha, N. K.; Qiao, G. G. High chain-end fidelity in sono-RAFT polymerization. *Polym. Chem.* **2022**, *13*, 6140–6148.
- (68) Bhangu, S. K.; Ashokkumar, M. Theory of Sonochemistry. In Sonochemistry: From Basic Principles to Innovative Applications; Colmenares, J. C., Chatel, G., Eds.; Springer International Publishing: Cham, 2017, pp 1–28.
- (69) Zaquen, N.; Rubens, M.; Corrigan, N.; Xu, J.; Zetterlund, P. B.; Boyer, C.; Junkers, T. Polymer synthesis in continuous flow reactors. *Prog. Polym. Sci.* **2020**, *107*, 101256.
- (70) Reis, M. H.; Leibfarth, F. A.; Pitet, L. M. Polymerizations in continuous flow: recent advances in the synthesis of diverse polymeric materials. *ACS Macro Lett.* **2020**, *9*, 123–133.
- (71) Hornung, C. H.; Guerrero-Sanchez, C.; Brasholz, M.; Saubern, S.; Chiefari, J.; Moad, G.; Rizzardo, E.; Thang, S. H. Controlled RAFT polymerization in a continuous flow microreactor. *Org. Process Res. Dev.* **2011**, *15*, 593–601.
- (72) Reis, M.; Gusev, F.; Taylor, N. G.; Chung, S. H.; Verber, M. D.; Lee, Y. Z.; Isayev, O.; Leibfarth, F. A. Machine-Learning-Guided Discovery of 19F MRI Agents Enabled by Automated Copolymer Synthesis. J. Am. Chem. Soc. 2021, 143, 17677–17689.

- (73) Taylor, N. G.; Reis, M. H.; Varner, T. P.; Rapp, J. L.; Sarabia, A.; Leibfarth, F. A. A dual initiator approach for oxygen tolerant RAFT polymerization. *Polym. Chem.* **2022**, *13*, 4798–4808.
- (74) Reis, M. H.; Varner, T. P.; Leibfarth, F. A. The influence of residence time distribution on continuous-flow polymerization. *Macromolecules* **2019**, *52*, 3551–3557.
- (75) Rubens, M.; Vrijsen, J. H.; Laun, J.; Junkers, T. Precise polymer synthesis by autonomous self-optimizing flow reactors. *Angew. Chem.* **2019**, *131*, 3215–3219.